Research Article

Mingwei Liu, Xiaolei Xue, Bikash Karmakar*, Waleed Eltantawy, Attalla F. El-kott, Emam M. El. Nashar, Eman M. Abd-Ella

Sonochemical synthesis of gold nanoparticles mediated by potato starch: Its performance in the treatment of esophageal cancer

https://doi.org/10.1515/chem-2023-0193
received June 14, 2023; accepted January 12, 2024

Abstract: Economically viable and eco-friendly potato starch (PS) was employed to synthesize Au NPs under ultrasound irradiation. PS phytochemicals have the function of a green reductant as well as an efficient stabilizer template to cap and synthesize gold nanoparticles. Transmission electron microscopy (TEM), UV-Vis spectroscopy, X-ray diffraction (XRD), scanning electron microscopy (SEM), and energy-dispersive X-ray spectroscopy (EDX) were applied to investigate the structure of the synthesized PS-Au NPs nanocomposite. FESEM results showed that the obtained Au NPs were spherical and ~30 nm in diameter; their crystalline nature was detected by XRD and TEM data. PS-Au NP nanocomposite shows high antioxidant effects against DPPH. The colorimetric MTT investigation was followed in the determination of anti-esophageal cancer properties of the PS-Au NP nanocomposite against KYSE-30 and FLO-1 cell lines. The findings indicate that in 3 days, the cancer cell survival percentage in various dilations reduced as much as the PS-Au NP nanocomposite concentration increased. The best anti-cancer effect of the PS-Au NP nanocomposite was reported at 1,000 μg/mL dilation. Through MTT cytotoxicity analysis the half-maximal inhibitory concentration of PS-Au nanocomposite or IC50 values against the KYSE-30 and FLO-1 esophageal carcinoma cells were found as 125 and 176 μg/mL, respectively. The data indicated that these PS-Au NP nanocomposites inhibited esophageal cancer cells more strongly than normal cells.

Keywords: Au nanoparticles, potato starch, DPPH, esophageal cancer

1 Introduction

The sustainable synthesis of noble metal nanomaterials has garnered significant interest because it is easy, accessible, inexpensive, nontoxic, and ecologically friendly as compared to other conventional methods. Additionally, this synthetic process can be used at standard pressure and temperature, which saves a significant amount of energy [1–4]. The process involves utilizing different plant components, such as root extract, encompassing seeds, leaf extract, stem extract, and fruit extract, which are employed in this process and act as reducing agents and stabilizers [3–7]. One of the primary uses is the creation of novel chemotherapeutic medications using metallic nanoparticles to treat a variety of malignancies, including those of the breast, lung, prostate, bone, and nerves [8–10]. Metallic nanoparticles enhance chemotherapy and reduce their side effects by directing drugs to target cancer cells [10–12]. They also allow surgery to be performed with greater precision and increase the effectiveness of radiation therapy and other current treatment options. The result of these activities is reducing the risk for the patient and increasing the probability of survival [12–16]. Between various metal oxide nanoparticles, Au NPs were more useful in the field of nanochemistry and nanomedicine due to their efficient anti-microbial, bacterial, and cancerous effects as well as their chemical stability [1–5]. Thus, green synthesis of these nanoparticles could be valuable in the field of pharmaceutical application. AuNPs, green-formulated by medicinal plants, have been

* **Corresponding author: Bikash Karmakar**, Department of Chemistry, Gobardanga Hindu College, 24-Parganas (North), India, e-mail: bikashkarm@gmail.com
Mingwei Liu, **Xiaolei Xue:** Department of Thoracic Surgery, Baoji Central Hospital, Baoji, 721008, China
Waleed Eltantawy: Department of Biology, Batterjee Medical College, Aseer 62451, Saudi Arabia
Attalla F. El-kott: Department of Biology, College of Science, King Khalid University, Abha 61421, Saudi Arabia; Department of Zoology, College of Science, Damanhour University, Damanhour, 22511, Egypt
Emam M. El. Nashar: Department of Anatomy, College of Medicine, King Khalid University, Abha, 62529, Saudi Arabia
Eman M. Abd-Ella: Department of Zoology, College of Science, Fayoum University, Fayoum, 65514, Egypt

applied for several types of cancers [11–13]. Based on previous studies, Au NPs remove the cancer cells by increasing the reactive oxygen species (ROS) levels in cells [10–12]. Also, other research studies have indicated the Au NP's role in entering the cancer cell membranes and killing them [10–13].

It has been suggested recently that carrier nanoparticles have the ability to mix and transport many anti-cancer medications. There are two ways to access this functionality. One way or another, resistance building in cancer cells is impeded when they come into contact with a particular kind of nanoparticle that includes multiple anti-cancer drugs [17–19] because there is extremely little chance of developing many mutations at once. Additionally, because various systems are exploited, combining many medications at once results in increased efficiency. In order to strengthen anti-cancer effects and avoid resistance, different kinds of nanoparticles might be used in combination [13,15].

Because of the potential uses of Au NPs in biomedical science and biotechnology, their production has drawn increased interest [1]. Researchers have utilized a diverse array of biological components, including microbes, plant extracts, starch, enzymes, and biopolymers, as natural reducing and stabilizing agents in the biosynthesis of these NPs [1–3]. Potato starch (PS) was selected here for the biogenic synthesis of Au NPs with the aid of ultrasonic energy (Scheme 1). PS presents itself as a potentially useful substitute template for the production of Au NPs because of its low toxicity and biodegradability, as well as its capacity to interact with metal ions and reduce them *in situ*. Prior to the synthesis, an array of analytical methods was used to examine the morphological and physicochemical characteristics of the produced PS-Au NPs. Towards the bio-application, the performance of the novel green nanomaterial was explored in restraining the esophageal cancer cells, i.e., KYSE-30 and FLO-1, being analyzed under *in vitro* conditions.

2 Experimental

2.1 Materials and methods

PS, $HAuCl_4$, NaOH, H_2O, and EtOH were purchased from Merck. Quartz cuvettes (10 mm) and a double-beam UV-Vis apparatus (PG, T80+) were utilized in the spectrophotometric studies in the spectral range of 220–700 nm with a resolution of 1 nm. FT-IR spectra were recorded on a Bruker VERTEX 80 V instrument, and the samples were made on KBr pellets. FESEM and EDX were performed to study the shape, sizes, and elemental compositions using TESCAN MIRA3 and TSCAN microscope, respectively. The

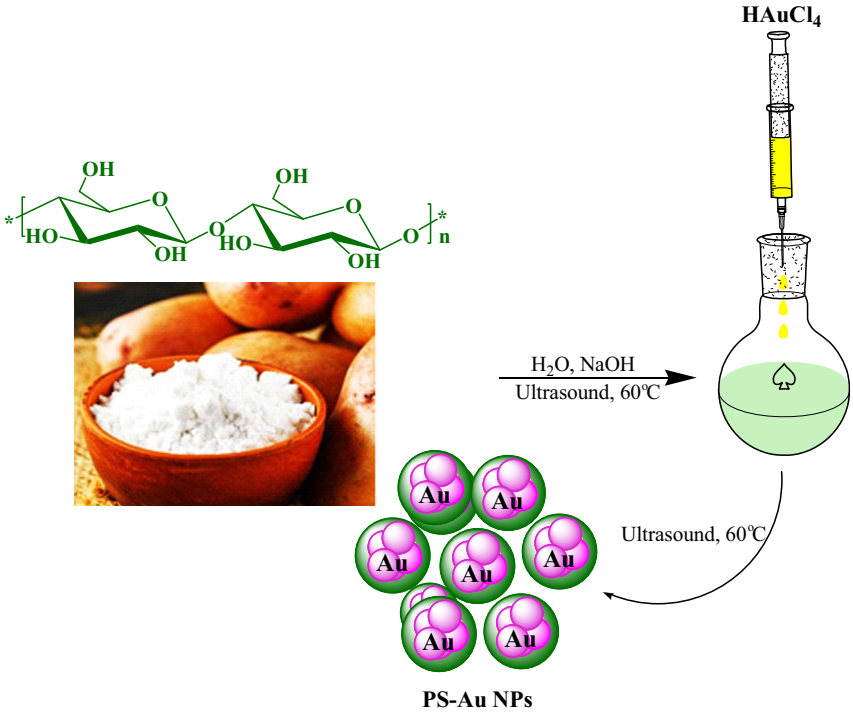

Scheme 1: Ultrasound-assisted preparation of PS-Au NPs.

samples were dispersed manually on a grid and gold layered before the study. Transmission electron microscopy (TEM) analysis was performed on a Phillips CM10 microscope at an accelerating voltage of 200 kV. Before the analysis, the sample dispersed on acetone was added as a drop over a carbon-coated Cu grid and dried prior to analysis. Powder X-ray diffraction (XRD) was carried out in the scanning range of 2θ = 10°–80° using Co Kα radiation (λ = 1.78897 Å) at 40 keV and a cathode current of 40 MA.

2.2 Preparation of PS solution

About 50 mL of DI water was used to dissolve nearly 0.2 g of PS powder, which was then sonicated for 2 min at room temperature. To get a clear solution for later use, Whatman No. 1 filter paper was used to filter it.

2.3 Synthesis of PS-Au NPs

About 1.5 mM $HAuCl_4$ solution in water (20 mL) was added to 20 mL of PS solution (1% w/v) in a beaker and stirred for 2 min. Then, the pH was maintained as 11 by the addition of NaOH solution (0.1 M) and sonicated in an ultrasonic bath (60 Hz) for 30 min at 60°C until a reddish solution was obtained (indicating the formation of Au NPs). The reddish-brown suspension mixture was centrifuged and washed repeatedly with water to obtain PS-Au NPs.

2.4 Antioxidant effects of the PS-Au NP nanocomposite

The antioxidant capacity of a substance is frequently determined by the DPPH method, where its potential to abstract the diphenyl-1-picrylhydrazyl (DPPH) free radical is assessed. It is a well-known colorimetric method based on free radical scavenging. The purple-colored alcoholic solution of DPPH is mixed with the experimental antioxidant sample, which is reduced by the free electrons or free hydrogen that results in quenching of its purple color to pale yellow. This change in absorption is observed using a UV-Vis spectrophotometer at 517 nm. The PS-Au NP nanocomposite was mixed in varied concentrations with equal volumes of DPPH in methanol, and BHT was used as a reference while comparing the corresponding outcomes. The % inhibition was determined using the following formula along with the corresponding IC_{50} values [20]:

$$\text{DPPH scavenging effect or inhibition}(\%) = [(\text{Ao} - \text{As})/\text{Ao}] \times 100,$$

where Ao is the absorbance of the reference and As is the absorbance of the samples.

2.5 Anti-esophageal cancer activity of the PS-Au NP nanocomposite

The DMSO solvent of nanoparticles in the MTT test has cytotoxic properties. To expurgate its activity on the treated cells, its amount should be less than 1% of the final solution. DMSO is toxic at a concentration of more than 1%, but it is nontoxic at less than 1%. The solution volume was eventually increased to 32 mL with the RPM11640 culture medium, which was added in 1 mL increments for improved dissolution. Then, the stock successive dilutions at ratios of 1:1, 1:2, 1:4, 1:8, 1:16, 1:32, 1:64, 1:128, 1:256, 1:512, and 1:1,024 and to prepare concentrations of 0–1,000 µg/mL were used [21]. The RPM11640 culture medium contained streptomycin (100 µg/mL), penicillin solution (100 U/mL), glutamine, and inactivated fetal bovine serum. After 3–4 passages, the cancer cells (KYSE-30 and FLO-1) and normal cells (HUVEC) were prepared in terms of morphology and number. After segregating the cells from the flask surface by trypsin-EDTA (Gibco BRL, Scotland), cell viability was assessed and counted, and 3×10^3 cells were cultured with or without nanoparticles in 96 wells. General characteristics and morphological changes of cells were evaluated after 1 day by Invert (Motic, AE31 model microscope, China).

The cytotoxicity effect of the nanoparticles was examined using MTT (methyl thiazol tetrazolium; Sigma-Aldrich, USA) colorimetric assay. Following a 24 h incubation period, a particular dose of the nanoparticle was added to the 96-well plates containing the cultured cells. Following a 48-h incubation period, a new culture containing MTT solution (20 µl/well) was added to the wells' culture medium, and the mixture was then incubated for 3 h at 37°C. Finally, the absorbance was read at a wavelength of 570 nm. Notably, three separate experiments were conducted to determine the impact of each nanoparticle concentration on the cancer cells; therefore, the numbers included in the figures are the average percentage of responses obtained in the inhibition of cell growth for three independent repetitions. According to the optical absorption values obtained by the ELISA

reader, the growth inhibition percentage associated with each dilation was assessed by the following formula [21]:

$$\text{Cell viability}(\%) = \frac{\text{Sample A}}{\text{Control A}} \times 100.$$

Finally, the amount of IC_{50}, which represents the nanoparticle concentration that inhibits the growth of cancer cells by 50%, was calculated through linear regression.

2.6 Statistical analysis

First, the normality of the data was tested using Minitab software, version 21. Then, the non-normal data were normalized. Data variance analysis was carried out using SPSS version 22 software, and graphs were drawn with the help of Excel software.

3 Results and discussion

3.1 Structural analysis of PS-Au NPs

Following a sustainable methodology for the bio-inspired synthesis of PS-encapsulated Au NPs (PS-Au NPs), they were characterized by various advanced analytical methods. When $HAuCl_4$ was mixed with the PS under ultrasound energy, the change in color from yellow to reddish brown was observed, which resembled the evolution of Au NPs, and it was established by UV-Vis spectrometry, as presented in Figure 1. Due to surface plasmon resonance, a band with a broad hump occurred at 542 nm that was recorded from the start of the reaction till 30 min. This indicates that bioreduction was accomplished by PS as a reducing agent.

The size, shape, and anatomy of the produced PS-Au NP nanocomposite were determined by electron microscopic techniques (FE-SEM and TEM). Figure 2 shows that the prepared Au NPs are quasi-spherical, with an average size of 25–30 nm. Due to the surface coating of Au NPs by starch biomolecules, the particle surface is quite rough. By

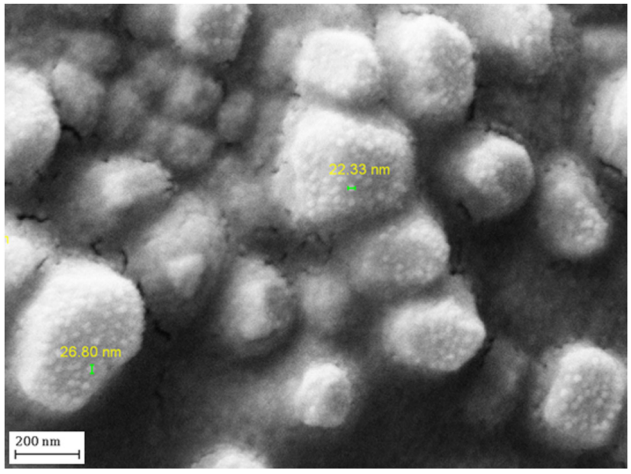

Figure 2: FE-SEM images of PS-Au NPs.

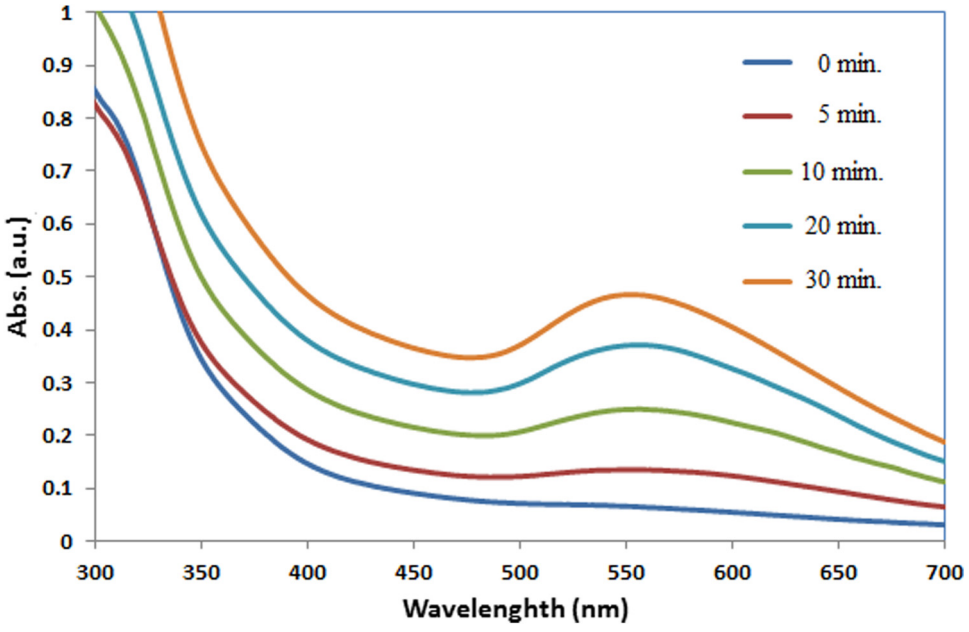

Figure 1: UV-Vis spectra of PS-Au NPs.

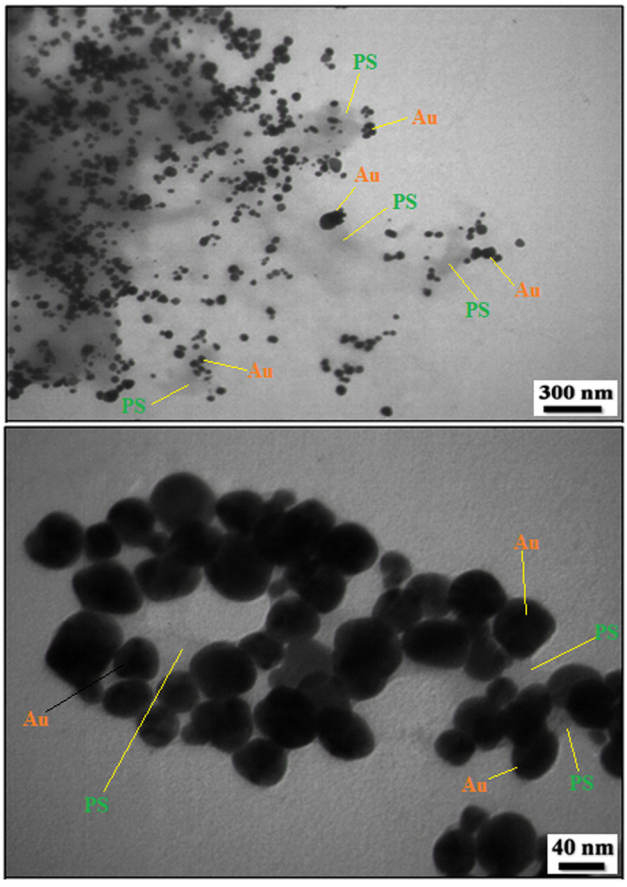

Figure 3: TEM images of PS-Au NPs.

using TEM analysis, the size and shape of the generated Au NPs were further examined (Figure 3) at different magnifications. It shows the gold nanoparticles are arranged in regular spherical geometry without any aggregations.

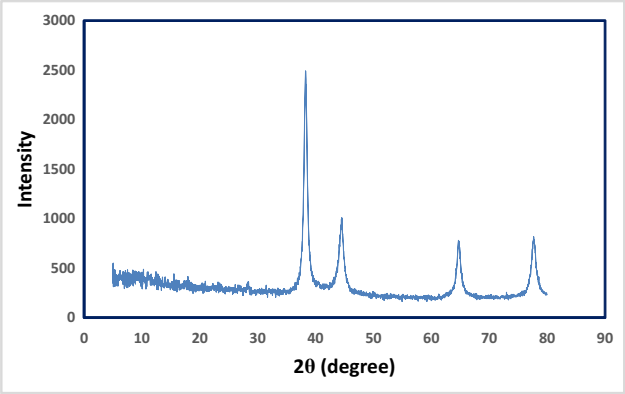

Figure 5: XRD patterns of PS-Au NPs.

The purity and elemental constitution of the synthesized PS-Au NPs were investigated by EDX analysis, as depicted in Figure 4. It shows that the maximum proportion of the elements is Au (93.6%). Also, in the lower pace, there are C (4.8%) and O (1.6%) atoms, corresponding to the PS polymer. These outcomes verified that the intended nanocomposite was produced successfully.

Figure 5 illustrates the crystallinity, purity, and phase behavior of the prepared PS-Au NP nanocomposite as examined by XRD analysis. The four observed reflection peaks at 2θ = 38.2° (111), 44.3° (200), 64.7° (220), and 77.4° (311) represent the synthesis of Au NPs in a face-centered cubic (fcc) state with a high crystalline nature.

Scheme 2 illustrates the structural coordination between Au^{3+} ions and starch biomolecules in an alkaline medium. The Au NPs initially formed are proposed to be capped over the polymeric starch, which is followed by a motivated nanocluster growth, as proposed by Ahmed and Emam [22].

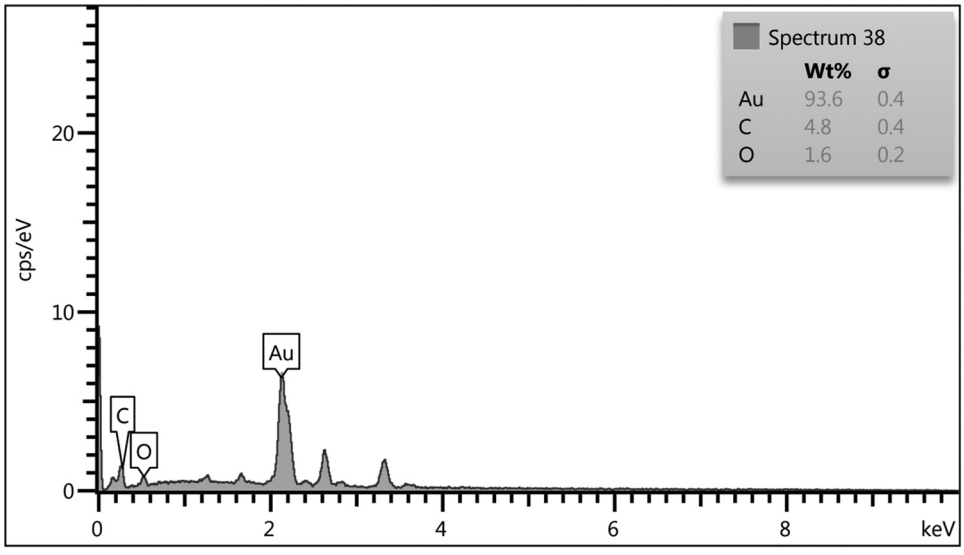

Figure 4: EDX analysis of PS-Au NPs.

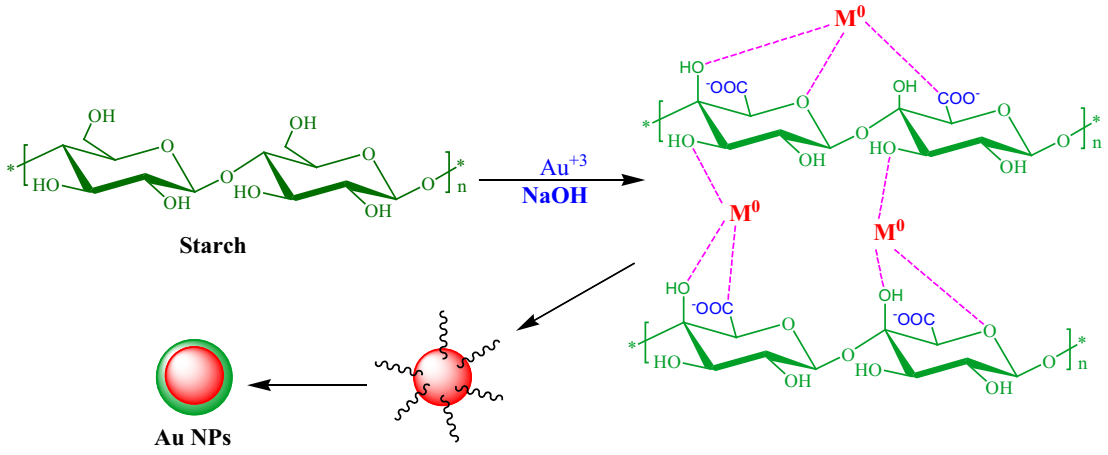

Scheme 2: Formation of Au NPs over starch.

It is suggested that the reducing hydroxyl functions of the starch backbone are exploited to reduce Au^{3+} ions to Au NPs, which are then meant to be oxidized to carbonyl groups. NaOH, a strong alkali, improved the starch's accessibility and reducibility and made it easier for the starch and gold ions to form coordinated bonds.

Starch was used to cap Au NPs, thus protecting them from oxidation and agglomeration. Investigations were conducted to study the impact of the reductant (starch) and precursor solution ($HAuCl_4$) concentrations on Au NPs. The findings show that these factors are crucial for the size and dispersibility of Au NPs as well as for their formation. It has been observed that when the quantity of Au salt is increased, the size of the Au NPs decreases along with time and starch content. We prepared smaller-sized Au NPs (10–20 nm), as shown in Figure 6, to compare their anti-cancer activity with larger-size (20–30 nm) Au NPs, as described in the current research.

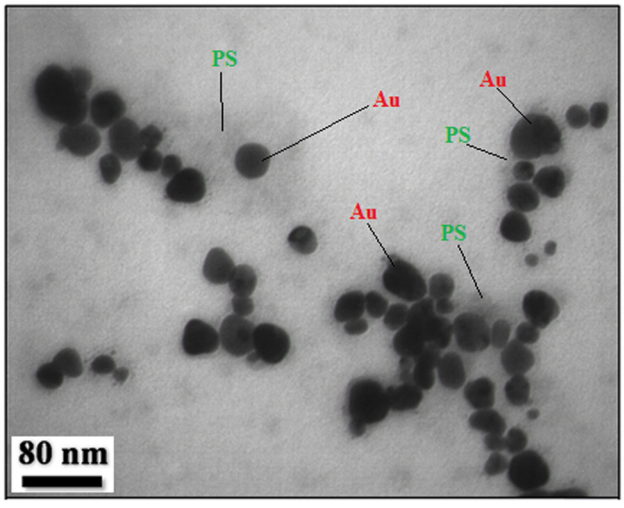

Figure 6: TEM images of PS-Au NPs.

Smaller Au NPs (4–20 nm) have a higher cytotoxicity efficacy compared to larger ones (20–28 nm), as suggested by Zhang et al. [23]. Therefore, we anticipate that our designed gold nanoparticles (10–20 nm) will have the best possible anti-cancer therapeutic effect. The corresponding cytotoxicity has been revealed in several cancer cells, such as MCF-7, Caco-2, MDA-MB-231, and Hep2 cancer cells [24–26]. The cytotoxicity of Au NPs is related to the functional groups, surface charge, and nanoparticle size [27]. The smaller size results in increased toxic effects, better cellular uptake, deep penetration inside specific tissues, and extensive tissue distribution [28]. Based on the above results, we observed notable anti-cancer efficacy of the formulated Au NPs at very low concentrations in both KYSE-30 and FLO-1 cells. The varied surface characteristics and smaller size of Au NPs could be the reasons for the observed notable anti-cancer effects.

3.2 Analysis of antioxidant capacity of the PS-Au NP nanocomposite

It is well reported that materials having significant anti-cancer properties and malignant cell apoptotic ability also exhibit momentous antioxidant potential. Therefore, along with cancer studies, we also investigated the antioxidant efficiency of the PS-Au NP nanocomposite following the DPPH radical scavenging assay associated with spectrometric analysis. The experimental material suspensions in several concentrations (0, 1, 3, 7, 15, 31, 62, 125, 250,

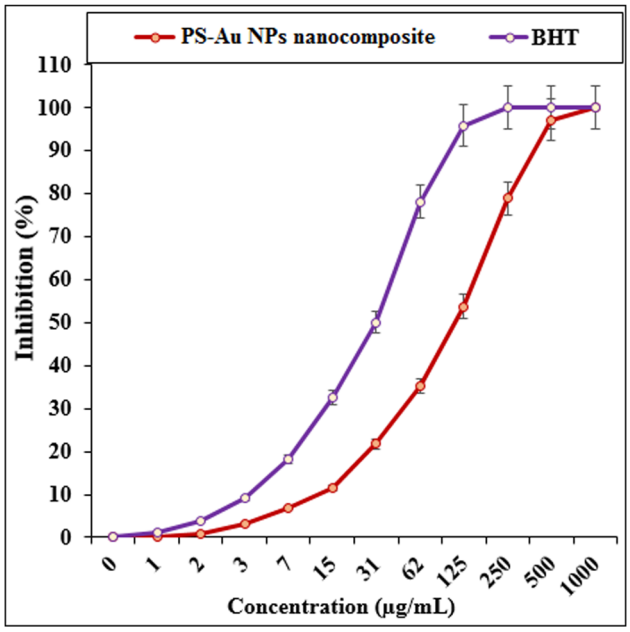

Figure 7: The antioxidant activities of the PS-Au NP nanocomposite and BHT.

500, and 1,000 µg/mL) were brought in contact with the ethanolic DPPH solution; the purple color gradually faded into pale yellow as the radical got quenched. UV absorption measurements, followed by the determination of % inhibition, were used to determine the antioxidant capacity of the material. Mechanistically, the DPPH free radical snatches the free protons or electrons from the PS-Au NP nanocomposite; as anticipated, the antioxidant material and the free radical pair up. The corresponding results are shown in Figure 7. Evidently, the inhibition (free DPPH radical inhibition %) values gradually decrease with an increase in the sample load and become lowest at 1,000 µg/mL, which is 0. The same trend is followed for BHT, too. The consequent IC_{50} values or the concentration of the antioxidant substance required for 50% quenching of the initial DPPH radical was determined, and the output is shown in Figure 6. While the standard BHT molecule exhibited an IC_{50} of 31 µg/mL, the PS-Au NP nanocomposite showed almost a comparable value of 113 µg/mL.

3.3 Anti-esophageal cancer effects of the PS-Au NP nanocomposite

Antioxidant substances with significant potential are prone to generate radical anions or active superoxide radicals, which are ultimately converted into ROS of different types, such as hydroxyl, nitric oxide, alkoxyl, alkyl, peroxyl, thiyl, and sulfonyl radicals. There are literature reports that demonstrate the considerable apoptotic ability of ROS to kill the proliferating cancer cells or at least restrain their unusual growth [29]. A disproportional increase in intracellular ROS can induce the arrest of the cancer cell cycle, which leads to an increase in mitochondrial oxidative stress. A second hypothesis is that the nanomaterial's sharp interfacial edges can promote the destruction of the cancer cell walls, finally causing the cell DNA breakdown [29]. Hence, during the cytotoxicity studies, when the PS-Au NP nanocomposite was brought in contact with the esophageal cancer cells (KYSE-30 and FLO-1), it strongly reduced the cell ATP content, finally leading to mitochondrial damage. The PS-Au NP nanocomposite is also able to generate ROS in high concentrations that would enhance cytotoxicity. In our studies, the cultured cells were treated with different concentrations of PS-Au NP nanocomposite, ranging from 0 to 1,000 µg/mL. After the necessary processing, as mentioned in Section 2.5, the MTT dye was introduced to each of the cell wells and processed again till the dissolution of the formazan crystals generated inside. The mechanism behind the formation of the purple formazan crystals is that the tetrazolium moiety reacts with the succinate dehydrogenase enzyme found in the mitochondrial membrane of living cells. Because they lack this enzyme, dead cells are unable to produce formazan and remain colorless when MTT is present. Finally, the spectrometric studies were followed, and the % cell viability was determined. The corresponding outcomes regarding the cytotoxic effects of the PS-Au NP nanocomposite against the KYSE-30 and FLO-1 cell lines have been demonstrated in terms of % cell viability in Table 1 and Figures 8 and 9. Markedly, the % cell viability is seen to decrease with the increasing loads of the cytotoxic material, PS-Au NP nanocomposite, in all the cell lines. Furthermore, we investigated the cytotoxic effects of the

Table 1: IC_{50} values of $HAuCl_4$ and the PS-Au nanocomposite in the cytotoxicity assay

	$HAuCl_4$ (µg/mL)	PS-Au NP nanocomposite (µg/mL)
IC_{50} against HUVEC	—	—
IC_{50} against KYSE-30	—	125 ± 0[a]
IC_{50} against FLO-1	—	176 ± 0[a]

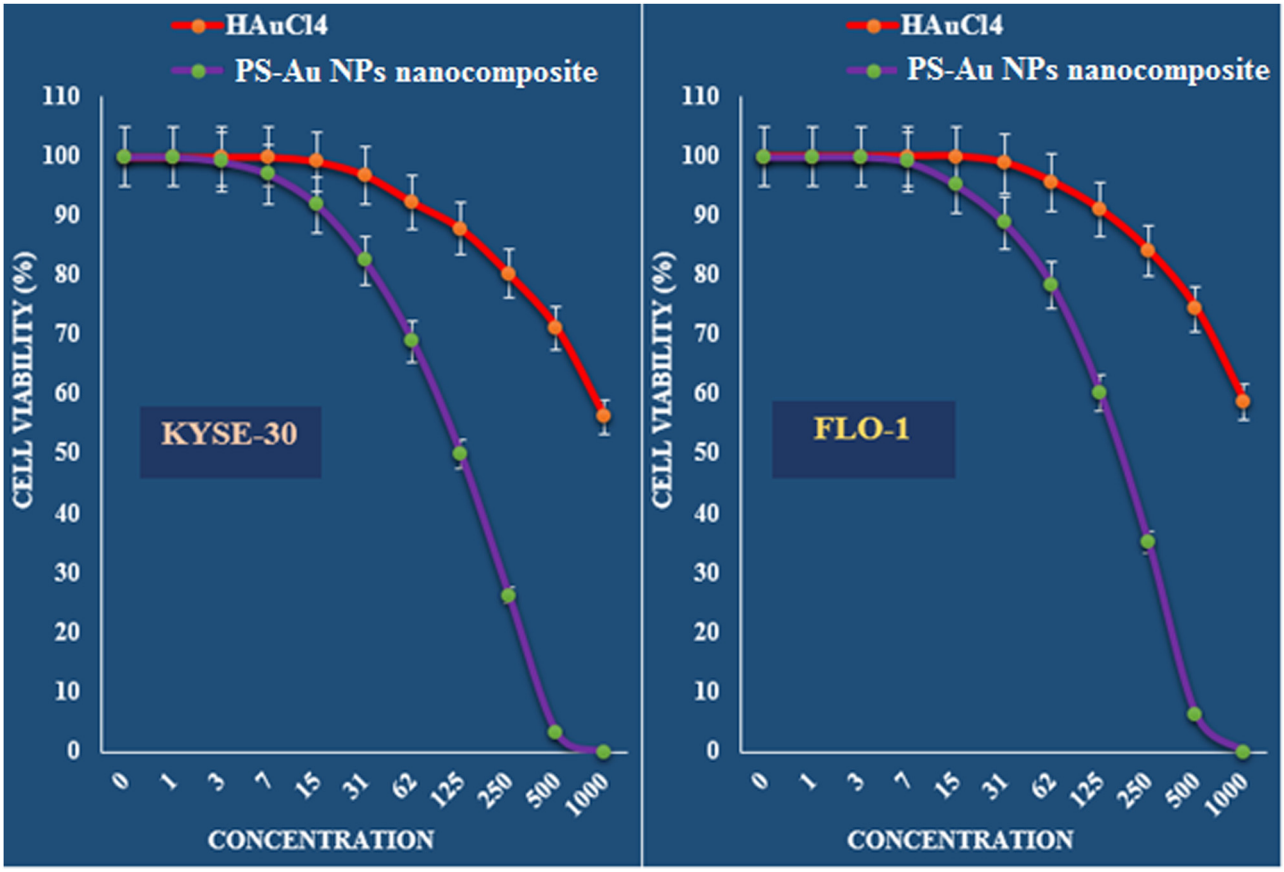

Figure 8: The anti-esophageal carcinoma properties (cell viability (%)) of $HAuCl_4$ and the PS-Au NP nanocomposite against KYSE-30 and FLO-1 cells.

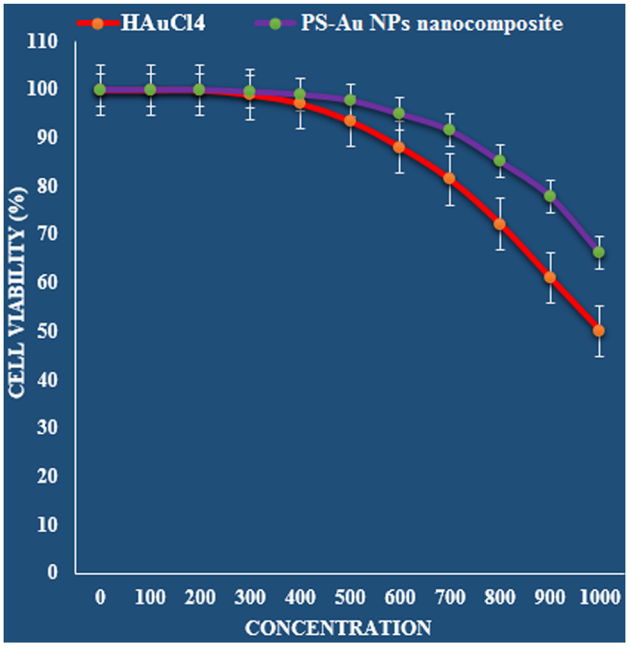

Figure 9: Cytotoxicity of $HAuCl_4$ and the PS-Au nanocomposite on normal (HUVEC) cells.

PS-Au NP nanocomposite over the normal cell line, HUVEC, to validate the adverse effects on the normal cells of the human body. Figures 8 and 9 show the corresponding profile where the material was studied in the same dose as applied in the earlier cell lines. However, no remarkable decrease of cell viability was observed. The corresponding IC_{50} values in the cancer studies are shown in Figures 8 and 9, where the concentrations of the sample material required to damage 50% of malignant cells were found as 125 and 176 µg/mL against the KYSE-30 and FLO-1 cells, respectively. As the values indicate, the best output was afforded by the KYSE-30 cell line, having the lowest IC_{50} value. Therefore, this study distinctly exhibits the considerable antiproliferative effect of the PS-Au NP nanocomposite on human esophageal cancer cells.

4 Conclusion

In summary, herein, we reported a novel bio-reduction procedure for the generation of Au NPs mediated by PS as a natural reducing and stabilizing agent under

ultrasonic energy to develop PS-Au NP nanocomposites with nano-medical application. The obtained Au NPs were 10–20 nm in diameter and spherical, as recorded by FESEM, and the crystallinity was ascertained by XRD and TEM analysis. After structural analysis, the PS-Au NP nanocomposite was analyzed for its antioxidant potential by DPPH radical scavenging assay, which displayed significant capacity compared to that of the standard BHT molecules. Next, the material was explored biologically to study cytotoxicity against human esophageal cancer cells using KYSE-30 and FLO-1 cell lines *in vitro* following MTT colorimetric analysis. The resultant IC_{50} values were calculated as 125 and 176 μg/mL for the above cell lines, respectively. Overall, the PS-Au NP nanocomposite was validated to be an effective nano-chemotherapeutic drug-like material for use against human esophageal cancer following *in vitro* studies.

Acknowledgement: The authors express their appreciation to the Deanship of Scientific Research at King Khalid University, Saudi Arabia, for funding this work through a research group program under grant number RGP. 1/428/44.

Funding information: The research was financially supported by King Khalid University (RGP. 1/428/44).

Author contributions: In terms of conception, data curation, formal analysis, acquisition, inquiry, methodology, project management, resources, software, supervision, validation, visualization, writing (original draft), and writing (review and editing), all authors played the same role.

Conflict of interest: The authors state that there is no conflict of interest.

Ethical approval: The experiments were conducted under *in vitro* conditions.

Data availability statement: The data obtained in the present research are available from the corresponding author upon reasonable request.

References

[1] Santra TS, Tseng FG, Barik TK. Green biosynthesis of gold nanoparticles and biomedical applications. Am J Nano Res Appl. 2014;2:5–12.

[2] Thakkar KN, Mhatre SS, Parikh RY. Biological synthesis of metallic nanoparticles. Nanomed: Nanotechnol Biol Med. 2010;6(2):257–62.

[3] Chokriwal A, Sharma MM, Singh A. Biological synthesis of nanoparticles using bacteria and their applications. Am J Pharm Tech Res. 2014;4(6):38–61.

[4] Saratale RG, Karuppusamy L, Saratale GD, Pugazhendhi A, Kumar G, Park Y, et al. A comprehensive review on green nanomaterials using biological systems: Recent perception and their future applications. Colloids Surf B Biointerfaces. 2018;170:20–35.

[5] Fariq A, Khan T, Yasmin A. Microbial synthesis of nanoparticles and their potential applications in biomedicine. J Appl Biomed. 2017;15(4):241–8.

[6] Pantidos N, Horsfall LE. Biological synthesis of metallic nanoparticles by bacteria, fungi and plants. J Nanomed Nanotechnol. 2014;5(5):1.

[7] Singh CR, Kathiresan K, Anandhan S. A review on marine based nanoparticles and their potential applications. Afr J Biotechnol. 2015;14(18):1525–32.

[8] Hulkoti NI, Taranath TC. Biosynthesis of nanoparticles using microbes-A review. Colloids Surf B: Biointerfaces. 2014;121:474–83.

[9] El Enshasy HA, El Marzugi NA, Elsayed EA, Ling OM, Malek RA, Kepli AN, et al. Medical and cosmetic applications of fungal nanotechnology: Production, characterization, and bioactivity. In Fungal nanobionics: Principles and applications. Singapore: Springer; 2018. p. 21–59.

[10] Yao Y, Zhou Y, Liu L, Xu Y, Chen Q, Wang Y, et al. Nanoparticle-based drug delivery in cancer therapy and its role in overcoming drug resistance. Front Mol Biosci. 2020 Aug 20;7:193.

[11] Qin L, Wu L, Jiang S, Yang D, He H, Zhang F, et al. Multifunctional micelle delivery system for overcoming multidrug resistance of doxorubicin. J Drug Target. 2018;26:289–95.

[12] Sui H, Zhou S, Wang Y, Liu X, Zhou L, Yin P, et al. COX-2 contributes to P-glycoprotein-mediated multidrug resistance via phosphorylation of c-Jun at Ser63/73 in colorectal cancer. Carcinogenesis. 2011;32:667–75.

[13] Viktorsson K, Lewensohn R, Zhivotovsky B. Apoptotic pathways and therapy resistance in human malignancies. Adv Cancer Res. 2005;94:143–96.

[14] Zhao Y, Huan ML, Liu M, Cheng Y, Sun Y, Cui H, et al. Doxorubicin and resveratrol co-delivery nanoparticle to overcome doxorubicin resistance. Sci Rep. 2016;6:35267. doi: 10.1038/srep35267.

[15] Zhao MD, Li JQ, Chen FY, Dong W, Wen LJ, Fei WD, et al. Co-delivery of Curcumin and Paclitaxel by "Core-Shell" targeting amphiphilic copolymer to reverse resistance in the treatment of ovarian cancer. Int J Nanomed. 2019;14:9453–67.

[16] Zhang S, Guo N, Wan G, Zhang T, Li C, Wang Y, et al. pH and redox dual-responsive nanoparticles based on disulfide-containing poly (β-amino ester) for combining chemotherapy and COX-2 inhibitor to overcome drug resistance in breast cancer. J Nanobiotechnol. 2019;17:109. doi: 10.1186/s12951-019-0540-9.

[17] Zang X, Zhao X, Hu H, Qiao M, Deng Y, Chen D. Nanoparticles for tumor immunotherapy. Eur J Pharm Biopharm. 2017;115:243–56.

[18] Xia S, Yu S, Yuan X. Effects of hypoxia on expression of P-gp and mutltidrug resistance protein in human lung adenocarcinoma A549 cell line. J Huazhong Univ Sci Technol Med Sci. 2005;25:279–81.

[19] Wang X, Liu X, Li Y, Wang P, Feng X, Liu Q, et al. Sensitivity to antitubulin chemotherapeutics is potentiated by a photoactivable nanoliposome. Biomaterials. 2017;141:50–62.

[20] Hemmati S, Heravi MM, Karmakar B, Veisi H. In situ decoration of Au NPs over polydopamine encapsulated GO/Fe_3O_4 nanoparticles as a recyclable nanocatalyst for the reduction of nitroarenes. Sci Rep. 2021;11:12362; Hemmati S, Heravi MM, Karmakar B, Veisi H.

Green fabrication of reduced graphene oxide decorated with Ag nanoparticles (rGO/Ag NPs) nanocomposite: A reusable catalyst for the degradation of environmental pollutants in aqueous medium. J Mol Liq. 2020;319:114302; Shahriari M, Sedigh MA, Mahdavian Y, Mahdigholizad S, Pirhayati M, Karmakar B, et al. In situ supported Pd NPs on biodegradable chitosan/agarose modified magnetic nanoparticles as an effective catalyst for the ultrasound assisted oxidation of alcohols and activities against human breast cancer. Int J Biol Macromol. 2021;172:55–61; Veisi H, Tamoradi T, Karmakar B, Hemmati S. Green tea extract–modified silica gel decorated with palladium nanoparticles as a heterogeneous and recyclable nanocatalyst for Buchwald-Hartwig C–N cross-coupling reactions. J Phys Chem Solids. 2020;138:109256–62.

[21] Hamelian M, Zangeneh MM, Amisama A, Varmira K, Veisi H. Green synthesis of silver nanoparticles using *Thymus kotschyanus* extract and evaluation of their antioxidant, antibacterial and cytotoxic effects. Appl Organomet Chem 2018;32:e4458; Hemmati S, Rashtiani A, Zangeneh MM, Mohammadi P, Zangeneh A, Veisi H. Green synthesis and characterization of silver nanoparticles using *Fritillaria* flower extract and their antibacterial activity against some human pathogens. Polyhedron. 2019;158:8–14; Hamelian M, Zangeneh MM, Shahmohammadi A, Varmira K, Veisi H. *Pistacia atlantica* leaf extract mediated synthesis of silver nanoparticles and their antioxidant, cytotoxicity, and antibacterial effects under *in vitro* condition. Appl Organometal Chem. 2020;34:e5278; Jalalvand AR, Zhaleh M, Goorani S, Zangeneh MM, Seydi N, Zangeneh A, et al. Chemical characterization and antioxidant, cytotoxic, antibacterial, and antifungal properties of ethanolic extract of *Allium Saralicum* R.M. Fritsch leaves rich in linolenic acid, methyl ester. J Photochem Photobiol B. 2019;192:103–12.

[22] Ahmed HB, Emam HE. Synergistic catalysis of monometallic (Ag, Au, Pd) and bimetallic (Agsingle bondAu, Ausingle bondPd) versus trimetallic (Ag-Au-Pd) nanostructures effloresced via analogical techniques. Mol J. Liq. 2019;287:110975. Emam HE, Ahmed HB. Comparative study between homo-metallic & hetero-metallic nanostructures based agar in catalytic degradation of dyes. Int J Biol Macromol. 2019;138:450–61; Ahmed HB, Mikhail MM, El-Sherbiny S, Nagy KS, Emam HE. pH responsive intelligent nano-engineer of nanostructures applicable for discoloration of reactive dyes. J Colloid Interface Sci. 2020;561:147–61; Emam HE, Saad NM, Abdallah AEM, Ahmed HB. Acacia gum versus pectin in fabrication of catalytically active palladium nanoparticles for dye discoloration. Int J Biol Macromol. 2020;156:829–40; Veisi H, Nasrabadi NH, Mohammadi P. Biosynthesis of palladium nanoparticles as a heterogeneous and reusable nanocatalyst for reduction of nitroarenes and Suzuki coupling reactions. Appl Organomet Chem. 2016;30:890.

[23] Zhang X-D, Wu D, Shen X, Liu P-X, Yang N, Zhao B, et al. Size-dependent in vivo toxicity of PEG-coated gold nanoparticles. Int J Nanomed. 2011;6:2071–81.

[24] Priya K, Iyer PR. Antiproliferative effects on tumor cells of the synthesized gold nanoparticles against Hep2 liver cancer cell line. Egypt Liver J. 2020;10(1):15.

[25] Majoumouo MS, Sharma JR, Sibuyi NRS, Tincho MB, Boyom FF, Meyer M. Synthesis of biogenic gold nanoparticles from Terminalia mantaly extracts and the evaluation of their in vitro cytotoxic effects in cancer cells. Molecules. 2020;25(19):4469.

[26] Jeyarani S, Vinita NM, Puja P, Senthamilselvi S, Devan U, Velangani AJ, et al. Biomimetic gold nanoparticles for its cytotoxicity and biocompatibility evidenced by fluorescence-based assays in cancer (MDA-MB-231) and non-cancerous (HEK-293) cells. J Photochem Photobiol B: Biol. 2020;202:111715.

[27] Kus-Liśkiewicz M, Fickers P, Ben Tahar I. Biocompatibility and cytotoxicity of gold nanoparticles: recent advances in methodologies and regulations. Int J Mol Sci. 2021;22(20):10952.

[28] Peng J, Liang X. Progress in research on gold nanoparticles in cancer management. Medicine (Baltimore). 2019;98(18):e15311.

[29] Grigalius I, Petrikaite V. Relationship between antioxidant and anticancer activity of trihydroxyflavones. Molecules. 2017 Dec;22(12):2169.